Self-assembly of neutral and ionic surfactants: An off-lattice Monte Carlo approach

Aniket Bhattacharya and S. D. Mahanti
Department of Physics, Michigan State University, East Lansing, Michigan 48824-1116

Amitabha Chakrabarti
Department of Physics, Kansas State University, Manhattan, Kansas 66506-2601

(Received 11 February 1998; accepted 16 March 1998)

We study self-assembly of surfactants in two dimensions using off-lattice Monte Carlo moves. Here the Monte Carlo moves consist of *slithering snake reptation* motion of the surfactant chains and *kink-jump* of the individual monomers. Unlike many previous studies an important feature of our model is that the solution degrees of freedom are kept implicit in the model by appropriate choice of the phenomenological interaction parameters for the surfactants. This enables us to investigate rather large systems with less number of parameters. The method is powerful enough to study *multimicellar* systems with regular and inverted micelles for both neutral and ionic surfactants. As a function of several parameters of the model, we study self-assembly of neutral surfactants into micelles of various forms and sizes and compute appropriate cluster-size distributions. Ionic surfactants exhibit, apart from micellization, additional *intermicellar ordering*. We further study the role of host particles to mimic recent experiments on surfactant-silicate cooperative self-assembly, and demonstrate the possibility of generalized pathways leading to host encased micellization. [S0021-9606(98)50124-9]

I. INTRODUCTION

Surfactants in solution are known to arrange themselves in a variety of structures, such as micelles, vesicles, and bilayers.[1–6] Design and fabrication of material composites can benefit from proper manipulation of these self-assembling properties of surfactants which may give rise to structural order over many length scales.[7] For example, semiconductor nanocrystals could be arranged in highly ordered structures by coating them with surfactants.[7] Synthesis of cobalt clusters by encapsulating them in inverted micelles is another example where self-assembling properties are used.[8] More recently this shape directing property has been exploited in synthesis of mesoporous sieves[9–13] where one can achieve large pore diameters which are structurally ordered over 100–200 Å with a similar level of perfection of well-established microporous solids of pore diameter in the range of only 5–10 Å. The organic surfactants are used as *templates* and the inorganic particles, usually silicates, encase the templating structure to produce organic-inorganic composite materials. Such self-assembling processes occur in all form of biological systems where it has been realized that organized organic arrays are an important part of inorganic nucleation and phase formations in biosystems known as *biomineralization*. Synthesis processes, such as ones mentioned above, quite naturally have relied on the central theme of biomineralization and have tried to use *biomimetic* approaches using supramolecular preorganized organic aggregates.[14]

Recent discoveries of mesoporous molecular sieves have made an important addition to this idea. Instead of using organic materials as a *passive* structure directing element, a more general pathway of *cooperative self-assembly* has been proposed[10,11] where the structure directing organic elements are allowed to dynamically evolve along with the inorganic host particles. This has lead to a wider tailoring capacity for structures which are not only ordered over larger length scales but the patterns and periodicity so obtained have opened up a wide arena to explore. Naturally, this generalized route of cooperative self-assembly[10,11] has gained widespread attention among scientific community for its prospective application in preparing nanoscale materials. The experimental pathways leading to such self-assembling structures are very diverse and complex. Each surfactant-host system in solution introduces competing interactions of different length scales arising out of different components. They involve hydrophobic and hydrophilic interactions, van der Waals interactions, Coulombic interactions and hydrogen bonding at different stages of the assembly process. A phenomenological model which captures these characteristics of surfactant-host self assembly via different pathways is naturally worthy of detail investigations.

The purpose of this article is twofold. First, to develop a phenomenological model for neutral and ionic surfactants which is particularly well suited for multimicellar system. We demonstrate that the proposed model captures the essentials of surfactant self-assembly for both neutral and ionic surfactants and is very efficient to study multimicelle systems. We then address the issue of cooperative self-assembly in presence of the host particles via different pathways. Before we describe our model and present our results it will be appropriate to summarize some of the relevant, previous work here. It is noteworthy in this context that a vast amount of literature has been addressed to the self-assembly of surfactants at the oil–water interface. For these three component

oil-water-surfactant systems we refer to the review article by Gompper and Schick[15] and references cited there.[16] In this article we focus on self-assembly of neutral as well as ionic surfactants immersed in one component solvent only. We then investigate the role of host particles in cooperative micellization of surfactants in their presence. Cooperative self-assembly of surfactants influenced by the presence of the host particles is a new subject of research and there exist only a few theoretical studies in the literature. Analytic treatments[4,17] of the self-assembly process quite often avoid the inherent complicated many body interactions and instead rely on space filling packing arguments. These calculations have been able to predict micellization and are very useful guides for further detailed numerical investigations. Due to their intrinsic complications, it is very hard to extend analytic approaches to more realistic models. But numerical work has been able to bridge the gap to some extent between many experiments and analytic theories. They can be broadly classified into two types. The first category deals with *realistic* systems with fairly large number of interaction parameters to mimic the actual structures and interactions of the surfactant molecules.[18,19] This class of models is better suited when one is interested in properties of an isolated macromolecule. But cooperative effects may appear at a late stage of the self-assembly process only after surfactants form micellar or aggregates of other shapes. Studies of dynamics of such processes may be severely restricted by computer resources if detailed geometries and the interactions are incorporated into the numerical scheme. The alternate route is to start with a simplified model emphasizing more macroscopic and universal properties, leaving aside the details but capturing the essence of the physical phenomena. We will adopt the second approach in this work. Surfactants interacting via simple Lennard–Jones (LJ) potential have been used as a paradigm for most of the previous lattice and off-lattice Monte Carlo (MC), and molecular dynamics studies.[20–26] The off-lattice simulations are to be compared with nearest neighbor lattice models both of which mimic *neutral* surfactants only. Desplat and Care[20] have performed lattice MC simulation where the surfactants consist of s particles with one of them serving as a head and the rest $s-1$ forming the tail of the surfactant. Their calculation qualitatively captures the micellar size distribution as a function of temperature. However since surfactants are embedded on a three-dimensional lattice it is not possible to extract information about the detailed shapes of the micelles. Equilibrium properties of nonionic micelles were also studied by Linse and co-workers and Mackie and co-workers by self-consistent field calculations and lattice Monte Carlo methods.[21] Rector *et al.* in their molecular dynamics (MD) simulations have adopted the simplest two particle model representing an amphiphile. In their treatment the surfactant consists of one hydrophilic and another hydrophobic particle only joined by a harmonic spring.[22] They also use a NpT ensemble and Widom test particle approach to determine the critical micelle concentration.[4] Smit *et al.* also established the presence of micelles in a surfactant-solvent mixture in their MD simulation.[23,24] Recent MD simulations by Palmer and Liu[25,26] are more detailed compared to those mentioned above. They have incorporated additional bending energy term and have considered surfactants of length 4 and 8, respectively, immersed in a solvent.[25] For a fixed set of parameters they observe cylindrical and spherical micellar assembly as a function of the surfactant concentration. They have also extended the calculation to take into account the inorganic precursors and concluded that beyond a critical surfactant-precursor interaction, the precursors have a deterring effect on preserving the shapes of the micelles. However since the solvent molecules are kept explicitly in their model, numerical results are restricted to only a few micelles and micelle–micelle interactions are almost negligible.[26]

In all of the numerical studies mentioned above, the solvent molecules are present explicitly in the calculations. However it is well known that for micellar self-assembly the ratio of surfactants to solvents is rather small and hence most of the computing efforts are spent towards monitoring the motion of the solvent particles. Therefore even for these models with simpler interactions it is hard to explore the phase diagram exhaustively. It will not be inappropriate to make some comments regarding the treatment of solvent degrees of freedom in earlier numerical studies of surfactant self-assembly. There have been many studies of the *hydrophobic effect* and *hydrophobic hydration*[4] which deal with the concomitant changes occurring at the microscopic structure of water in the vicinity of surfactants.[27] Experimentally however micellar aggregation have also been seen in other solvents which indicate that self-assembly may not require the detailed nature of the interaction of surfactants with water. Previous numerical simulations which capture the essential features of micellar aggregation also model the solvent with simple LJ potential. Hence one may think that the length scales associated with detailed nature at the molecular level contribute relatively weakly and those have been integrated out in simple models of surfactant-solvent systems cited above. Unlike many previous numerical studies of surfactant self-assembly, an important ingredient of our approach is that we have gone one step further and have effectively eliminated the solvent degrees of freedom completely. The effect of the solvent has been indirectly incorporated by appropriate set of phenomenological parameters among the surfactants. Evidently the model as we will describe in the next section contains less number of phenomenological parameters and the method has considerable computational advantages. For a range of parameters we observe micellar aggregation with similar cluster size distribution as found in earlier studies for neutral micelles where the solvent degrees of freedoms were incorporated explicitly. Next we have shown that *inverted micelles* and their distribution functions come naturally into this scheme. We then extend these studies for *ionic surfactants* by incorporating additional screened Coulomb (SC) interaction among the head groups of the surfactants. Apart from micellization, *ionic micelles exhibit additional structural ordering*. Finally, we present results for host encased micellization as a demonstration of *cooperative self-assembly* alluded to above.

II. MODEL

Our model consists of the surfactants and the host particles only, but the interaction potentials describing the surfactants in our model are similar to those used in previous studies. In this article we consider a two-dimensional model. This captures the basic features of self-assembly and enables us to search the parameter space more exhaustively. The model surfactant consists of chains of length N_m ($N_m=7$) of which the first one or two are chosen to be head (h) sites ($N_h=1$ or 2) and the rest of the monomers are treated as tails (t) sites. We consider surfactant chains of fixed bonds of unit lengths ($l_0=1$) but introduce bond bending energy. The potential function for the model is then given by:

$$U=\sum_{i<j}^{N}\phi_{ij}(r_{ij})+\sum R_b(\theta_{ijk}-\theta_0)^2, \tag{1}$$

where r_{ij} is the distance between sites i and j, θ_{ijk} is the angle subtended by three successive monomers in a given surfactant, and θ_0 is the equilibrium value of θ_{ijk}. In our calculations we have chosen $\theta_0=\pi$ but kept R_b as a parameter.[28] Note $\phi_{ij}(r_{ij})$ is a pairwise potential acting between any two monomers and is of LJ form:

$$\phi_{ij}(r_{ij})=\begin{cases}4\epsilon_{ij}\left[\left(\dfrac{r_{ij}}{\sigma_{ij}}\right)^{12}-\left(\dfrac{r_{ij}}{\sigma_{ij}}\right)^{6}\right]-\phi_0(R_{ij}^c), & r_{ij}<R_{ij}^c\\ 0, \quad r_{ij}\geqslant R_{ij}^c.\end{cases} \tag{2}$$

Here ϵ_{ij}, σ_{ij}, and R_{ij}^c are the LJ parameters and cutoff distances for the pair of monomers i and j, respectively. The addition of the term $\phi_0(R_{ij}^c)$ causes the interaction to vanish smoothly at a distance $R_{ij}^c\sigma_{ij}$ and beyond. In order to model surfactants in a solvent one needs two values of the cutoff parameter R_{ij}^c. A cutoff $R_{ij}^c=2^{1/6}\sigma_{ij}$ introduces a purely repulsive interaction, whereas a choice of $R_{ij}^c=2.5\sigma_{ij}$ introduces an attractive LJ tail. In this article we consider surfactants with hydrophilic heads and hydrophobic tails. Therefore when these surfactants are in water there is an effective attraction among the hydrophobic tails, a head-tail and a head-head repulsion. In our method these could be modeled with appropriate cutoff parameters $R_{hh}^c=2^{1/6}\sigma_{hh}$, $R_{ht}^c=2^{1/6}\sigma_{ht}$, and $R_{tt}^c=2.5\sigma_{tt}$, respectively. To model the host particles (p) we choose simple monomers interacting among themselves and with the surfactants with LJ potential. The interaction of the host particles among themselves and with the heads are taken to have both repulsive and attractive parts. However the strengths of the interaction ϵ_{pp} and ϵ_{hp} are in general different. The interactions of the host particles with the tails are always repulsive. Units of length and the temperature (T) have been chosen as σ_{tt} and ϵ_{tt}/k_B, respectively.

For ionic surfactants there is an additional SC interaction among the heads. We use the standard Debye-Huckel (D-H) form[4] given by

$$U_{ij}^{sc}(r_{ij})=u_0\,\frac{\exp(-\kappa r_{ij})}{r_{ij}}, \tag{3}$$

where the interaction strength κ^{-1} is the D-H screening length and u_0 is a function of the total charge of a surfactant. We will use u_0 and κ as phenomenological parameters. We should also state that there are counterions in the solvent for charge neutrality which contribute to the screening but do not appear in our calculations explicitly.

The Monte Carlo moves consist of off-lattice counterparts of forward and backward *slithering-snake* reptation moves[29] of the surfactants, and *kink jumps*[30] of the individual monomers. In one forward reptation move a given surfactant is chosen at random and is translated by an amount $\sim l_0$ in any direction. A kink jump is the off-lattice counterpart of the Verdier-Stockmeyer model[30] which consists of putting the inner ith particle to its mirror image position along the bond joining its adjacent monomers satisfying the following equation:

$$\mathbf{R}_i'=\mathbf{R}_{i+1}+\mathbf{R}_{i-1}-\mathbf{R}_i, \tag{4}$$

and the end particles are then rotated according to

$$\mathbf{R}_1'=\mathbf{R}_2+\boldsymbol{\psi}_1$$
$$\mathbf{R}_{N_m}'=\mathbf{R}_{N_m}+\boldsymbol{\psi}_m, \tag{5}$$

where $\boldsymbol{\psi}_1$ and $\boldsymbol{\psi}_m$ are two randomly chosen vectors of length $l_0=1$.

A single *reptation* causes the whole surfactant to move whereas a single kink jump makes one monomer to flip only. Therefore a single MC step in our model consists of one reptation and N_m-1 kink jumps chosen at random. Periodic boundary conditions are applied and a link list[31] is used for MC updates. However the link list used here is different than the one often used in MD. When a given move is accepted, the neighbor list for that and the neighboring cells is updated immediately. In order to calculate the energy change for the reptation it is not necessary to calculate the energy change for all the N_m monomers in that chain. A careful observation shows that the change in energy is given by

$$\Delta E=[e_1'+e_{N_h+1}']-[e_{N_h}+e_{N_m}], \tag{6}$$

where e_i and e_i' correspond to the energy of the ith monomer for the old and the new configurations, respectively. The new configurations are accepted by the standard Metropolis rule. Now we will discuss our simulation results.

III. RESULTS

A. Thermodynamic considerations

Before we describe our results let us first briefly review some of the earlier analytic results due to Israelachvili and co-workers.[4,17] For other detailed work we refer the reader to the work of Blankschtein and co-workers,[32] and Ben-shaul and co-workers.[33] An important quantity in the theory of cluster aggregation is the dependence of chemical potential on aggregation number N. Equilibria among different aggregates imply

$$\mu=\mu_1^0+kT\,\log(X_1)$$
$$=\mu_2^0+\frac{1}{2}\,kT\,\log\left(\frac{X_2}{2}\right)=\cdots=\mu_N^0+\frac{kT}{N}\,\log\left(\frac{X_N}{N}\right) \tag{7}$$

or

$$\mu = \mu_N = \mu_N^0 + kT \log\left(\frac{X_N}{N}\right) = \text{const}, \quad N = 1,2,3,... \tag{8}$$

where μ_N is the mean chemical potential of the aggregate of aggregation number N and μ_N^0 is the standard part of the chemical potential. Note X_i/i is the mole fraction of the ith species so that the total concentration C of surfactants is given by

$$\sum_{i=1}^{\infty} X_i = C. \tag{9}$$

From Eq. (7) it is easy to get the following equation:

$$\frac{X_N}{N} = \left[X_1 \exp\left(\frac{\mu_1^0 - \mu_N^0}{kT}\right)\right]^N. \tag{10}$$

The above equation gives the necessary conditions for the aggregates to form. Since $X_i < 1 \ \forall i$, it follows that if μ_i^0 is a constant

$$\frac{X_N}{N} = X_1^N \ll 1. \tag{11}$$

In other words $X_N/N \ll X_1$, so that the large aggregates are rare. It generally follows that in order to get aggregates of appreciable size, μ_N^0 has to decrease as a function of N. An important aspect of this functional dependence is micellization versus complete phase separation. Israelachvili and coworkers have shown that if $\mu_N^0 = \mu_\infty^0 + A/N^p$ then for $p<1$ there is a phase separation. It is noteworthy that in this case μ_N^0 goes to μ_∞^0 at large N. Micellization on the contrary will occur if μ_N^0 either exhibits a minimum, or becomes constant for finite aggregation number N. For surfactants forming spherical micelles, a reasonable assumption is that the attractive energy among the hydrophobic tails is proportional to the surface area γa and the repulsive contribution arises due to the hydrophilic head groups is proportional to K/a so that

$$\mu_N^0 = \gamma a + \frac{K}{a}, \tag{12}$$

where a is the effective surface area that a surfactant occupies at the surfactant–solvent interface.[34] These two opposing terms immediately give a minimum in μ_N^0 at the optimal surface area $a_0 = \sqrt{(K/\gamma)}$. The validity of this simple thermodynamic and geometric packing argument can be compared with the cluster statistics obtained from our simulation results. In our simulation we have calculated average energy per surfactant chain $\tilde{E}_N$ for a cluster of aggregation number N. We will see that $\tilde{E}_N$ is a very useful quantity to understand the underlying physics of micellization. The dependence of $\tilde{E}_N$ on the aggregation number N, bending coefficient R_b, and T is extremely useful in tailoring shapes and sizes in the aggregation process.

B. Neutral surfactants

We first present results for the neutral surfactants. Our model of neutral surfactant consist of chains with $N_m = 7$ where the first two sites are considered as head sites and the rest of the monomers consist of the tail particles. The LJ parameters are summarized in Table I. The simulation is performed for 200 surfactant chains ($N_c = 200$) confined in a square box of length 100 so that the surfactant concentration[35] (number of surfactants per unit area) is 0.02. Initial configurations are generated by first choosing the sites for the surfactant heads randomly and generating the rest of the chain particles with an off-lattice two-dimensional self-avoiding walk. We then equilibrate the system with purely repulsive interaction for all the particles. This makes the surfactants to be uniformly distributed. We explore the phase diagram at this fixed concentration as a function of temperature (T) and bending energy parameter R_b.

TABLE I. Interaction parameters for the neutral surfactants.

Interaction	R_{ij}^c/σ_{ij}	σ_{ij}	ϵ_{ij}
Head-head	$2^{1/6}$	1.0	1.0
Head-tail	$2^{1/6}$	1.0	1.0
Tail-tail	2.5	1.0	1.0

First we show some typical snapshots that we get from the off-lattice simulation of surfactants without explicit incorporation of the solvent particles. We have investigated surfactant self-assembly for a wider range of T and R_b. Here we show only some of the most relevant results. Figure 1 shows typical snapshots of micellar aggregation after 500 000 MC steps for $T = 0.5$ and for different values of the bending energy parameter (R_b). We notice with increasing the value R_b from 0.1 to 1.0, the shapes of the clusters change from circular to more rectangular structures. We will come back to this issue later. In order to understand the effect of each parameter on micellization in detail we have relied on two quantities. The first one is the average energy per surfactant chain $\tilde{E}_N$ for aggregates of given size N. The second quantity is the corresponding cluster distribution function for which we have used a simple distance criterion to determine whether a surfactant belongs to a given cluster. For hydrophobic tails, two surfactant chains are considered in the same cluster if any two pair of monomers from these two surfactant tails lie within the attractive cutoff distance (2.5). In order to determine $\tilde{E}_N$ and the cluster distribution function an ensemble average is taken over three to six sets of independent runs. For higher temperature we have checked that statistics for two independent runs are almost identical. A time averaging on the cluster distribution is performed over different time windows. Invariance of these cluster distributions ensures that a steady-state distribution has been achieved.

Figure 2 shows typical snapshots of micellar aggregation for the temperatures 0.8, 0.6, 0.45, and 0.4, respectively, for $R_b = 0.2$ and in Fig. 3 we show the corresponding time averaged cluster distribution functions for the entire run (circles), for the last 100 000 (squares), and the last 50 000 (diamonds), respectively, by calculating the distribution function in every 500 MC steps. The squares and the circles are almost in identical position and therefore can be interpreted as the steady-state cluster distribution. The circles may be relevant for those experiments where data is taken for the entire span of the experiments. At higher temperature the cluster

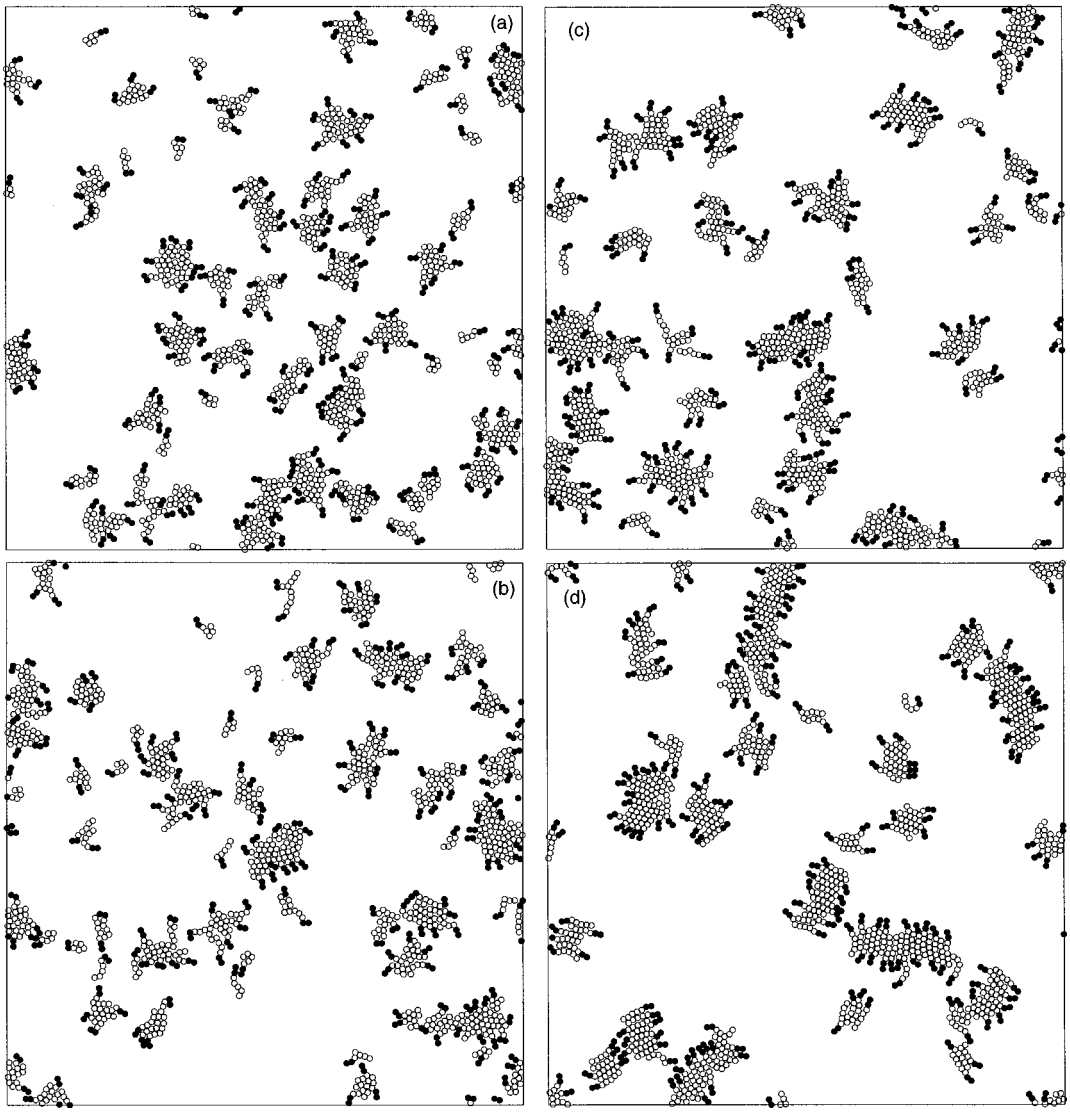

FIG. 1. Snapshots of micellar aggregation for a 2% surfactant solution with chain length $N_c=7$ at a temperature 0.5 (in reduced unit) at the end of MC time 500 000. The MC simulations were done for 1400 monomers confined in a two-dimensional box of length 100 (in units of LJ parameter σ) with periodic boundary conditions along both x and y directions. The figure shows snapshots for different values of R_b: (a) $R_b=0.1$, (b) $R_b=0.2$, (c) $R_b=0.6$, and (d) $R_b=1.0$.

distribution decreases monotonically. As the temperature is lowered the cluster distribution exhibits a peak. Figure 3(c) is very similar to the cluster distribution observed in previous simulations with explicit solvent degrees of freedom. It is characterized by a large number of free surfactant chains and a characteristic peak at a larger value of N. We should mention that while the cluster distributions remain in a steady state, breaking of clusters into pieces and coalescence of smaller clusters proceed simultaneously with aggregates of different sizes being in chemical equilibrium with each other. A time development of such events is shown in Fig. 4 for a particular set.

We now discuss the N dependence of $\tilde{E}_N$. Figure 5 shows the $\tilde{E}_N$ as a function of N at different temperatures. Figure 5 should be compared with Fig. 3 which shows the corresponding cluster distributions. Here we notice an important result. For micellization, the dependence of $\tilde{E}_N$ on N has to become flat at a finite N, or as a function of N exhibit a minimum.[36] We notice in Fig. 3 that at a temperature of 0.8, the distribution comprises mostly of monomers as it is apparent from the scale of Fig. 3(a). The corresponding plot for $\tilde{E}_N$ also monotonically decreases with N. According to the simple theory *a la* Tanford and Israelachvili *et al.* sketched above,[3,4] a minimum (at $N=M$, say) occurs because of the competition of the attractive and repulsive units in the surfactants. For $N<M$ the hydrophobic energy is increased where as for $N>M$, the geometric constraint increases the free energy. For higher temperature the thermal energy is of the same order of magnitude of the attractive interaction energy ($\epsilon_{tt}=1$) and hence the system effectively behaves as a purely repulsive one. With decrease of temperature the attractive interaction overcomes the thermal effect and a minimum appears in $\tilde{E}_N$ as shown in Figs. 5(b) and 5(c). With further decrease of temperature the energy landscape for $\tilde{E}_N$ becomes more rugged exhibiting multiple minima. Our simulations very clearly demonstrate the key

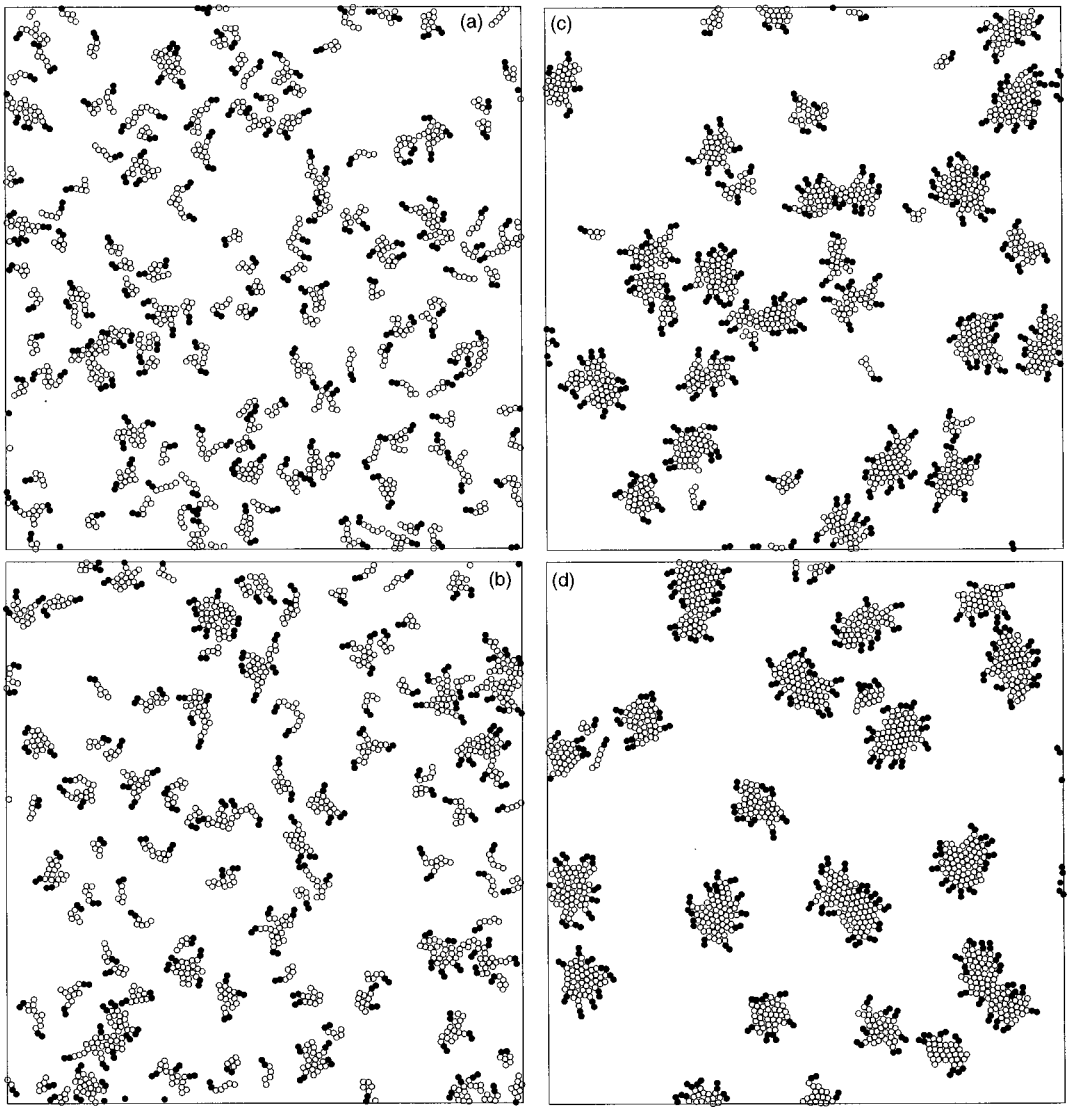

FIG. 2. Snapshots of micellar aggregation for a 2% surfactant solution with chain length $N_c=7$ for $R_b=0.2$ and for temperatures 0.8, 0.48, 0.45, and 0.4 (in reduced unit), respectively, at the end of MC time 500 000. The MC simulations were done for 1400 monomers confined in a two-dimensional box of length 100 (in units of LJ parameter σ) with periodic boundary conditions along both x and y directions.

features of the physical processes controlling micellization. One needs an attractive interaction which can overcome thermal fluctuations and a repulsive steric repulsion for modeling micellization of surfactants. We should mention that unlike earlier simulations with explicit solvent degrees of freedom, our effective LJ parameters should be considered as temperature dependent when one takes into account the effect of the implicit solvent condition as the temperature changes.

Next, we have studied the the effect of R_b on micellization. From Fig. 1 it is clear that by increasing R_b, the shape of the micelles gradually changes from being spherical to rectangular structures. For comparison with Fig. 2(c) ($T=0.45$, $R_b=0.2$) we have shown another snapshot for the same temperature bur for $R_b=0.6$ in Fig. 6(a). A comparison of Fig. 2(c) and Fig. 6(a) very clearly shows how the bond-bending energy influences the shapes of the micelles. The cluster distribution and the $\tilde{E}_N \sim N$ is also qualitatively different. A larger bending energy introduces polydispersity in the cluster distribution as shown in Fig. 6(b). Again one can see how it occurs from the $\tilde{E}_N \sim N$ plot shown in Fig. 6(b). Comparing Fig. 6(c) with the corresponding Figs. 3(c) and 5(c) (for $T=0.45$) we notice that Fig. 6(a) lacks a sharp minimum, it contains multiple shallow energy valleys instead. This could be qualitatively understood by looking at the configurations of Fig. 6(c). With a larger value of R_b the surfactants arrange themselves in a rectangular shape. In an ideal situation for a very large bending energy the shape of the individual surfactants will be dominated by bending energy and therefore individual surfactants will become rod-like. Therefore the cluster energy will be minimized by arranging the surfactants such that heads of the alternate surfactants lie on one side. It is then easy to check that the cost of putting one more surfactant will be roughly the same as the average surfactant energy in that cluster, or in other words $\tilde{E}_N \sim \tilde{E}_{N+1}$, which implies that the $\tilde{E}_N$ vs N will exhibit plateaus. What we have just stated is true in the ideal limit for very large aggregates and for infinitely rigid rod

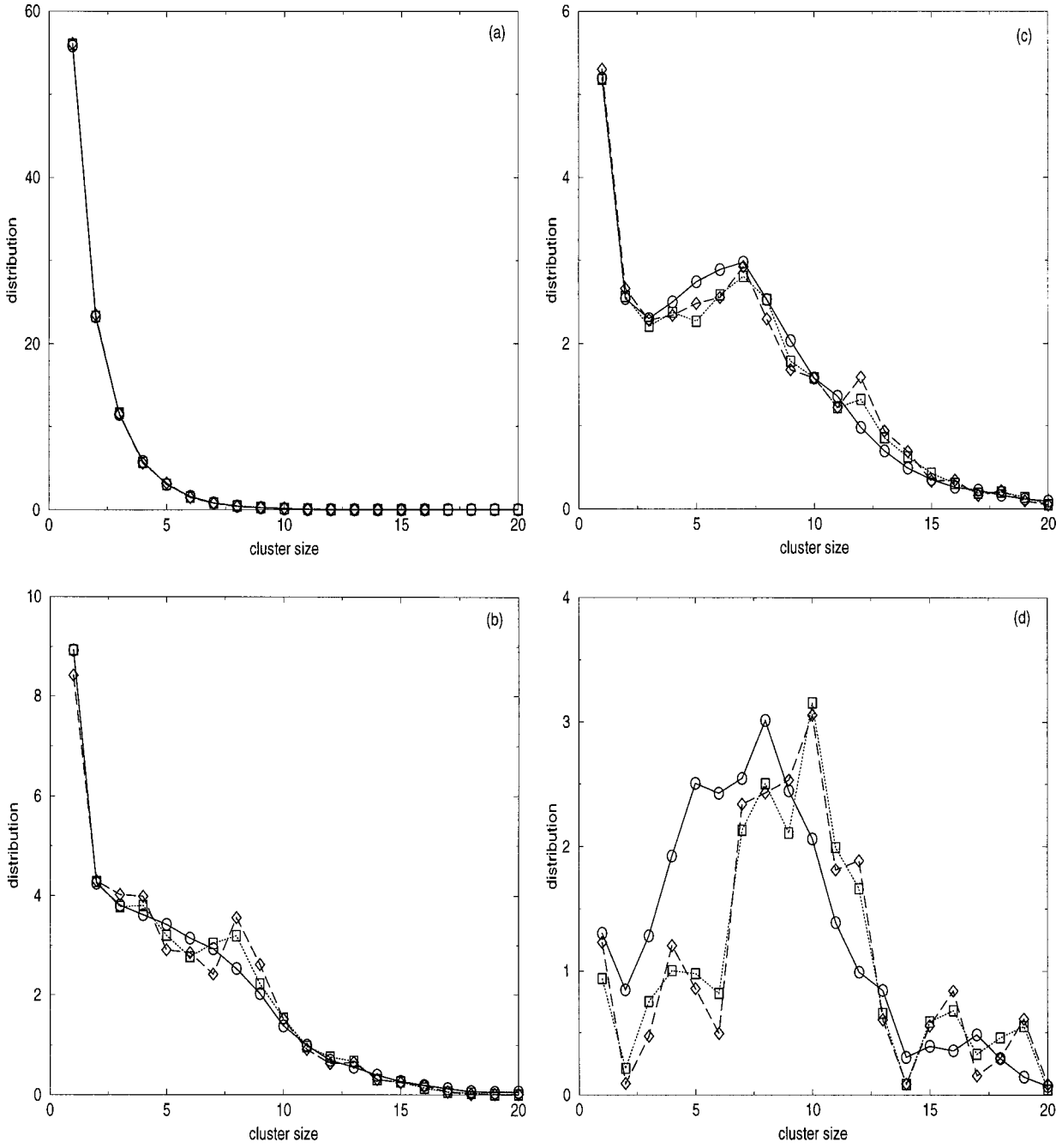

FIG. 3. Cluster size distributions for Figs. 2(a)–2(d). Circles represent the time averaged distribution for the entire run. Squares and diamonds represent time averaged distribution for the last 100 000 and 50 000 time steps. The ensemble average is performed over three to six different initial configurations.

shaped surfactants. In our case the above argument will be modified by the surface effects and also by the finite value of the bending energy which is reflected in Fig. 6(c), where one sees a relatively flat $\tilde{E}_N \sim N$ compared to that in Fig. 5(c). These studies show how the rigidity of the surfactants (controlled through R_b) can introduce polydispersity on micellization. An important aspect of our numerical results is the plot $\tilde{E}_N \sim N$ as a function of T and R_b which explains why cluster distributions in various cases are different.

C. Inverted micelles

Since our model captures the regular micellization process, it is almost self-evident how one obtains inverted micelles in this scheme. For the sake of completeness we will briefly describe it here. Surfactants with attractive heads and repulsive tails produce inverted micelles as expected. Thus, inverted micelles can be obtained with the following choice for the cutoff parameters $R_{hh}^c = 2.5\sigma_{hh}$, $R_{tt}^c = 2^{1/6}\sigma_{tt}$, $R_{ht}^c = 2^{1/6}\sigma_{ht}$. Figure 7 shows a typical snapshot and the corresponding distribution function.

D. Ionic surfactants

We now show results for the ionic surfactants. Our model ionic surfactant consists of one head and six tail particles. Ionic heads are taken to be bigger[37] than the tail particles with a choice $\sigma_{hh} = 2\sigma_{tt}$ which leads to a natural

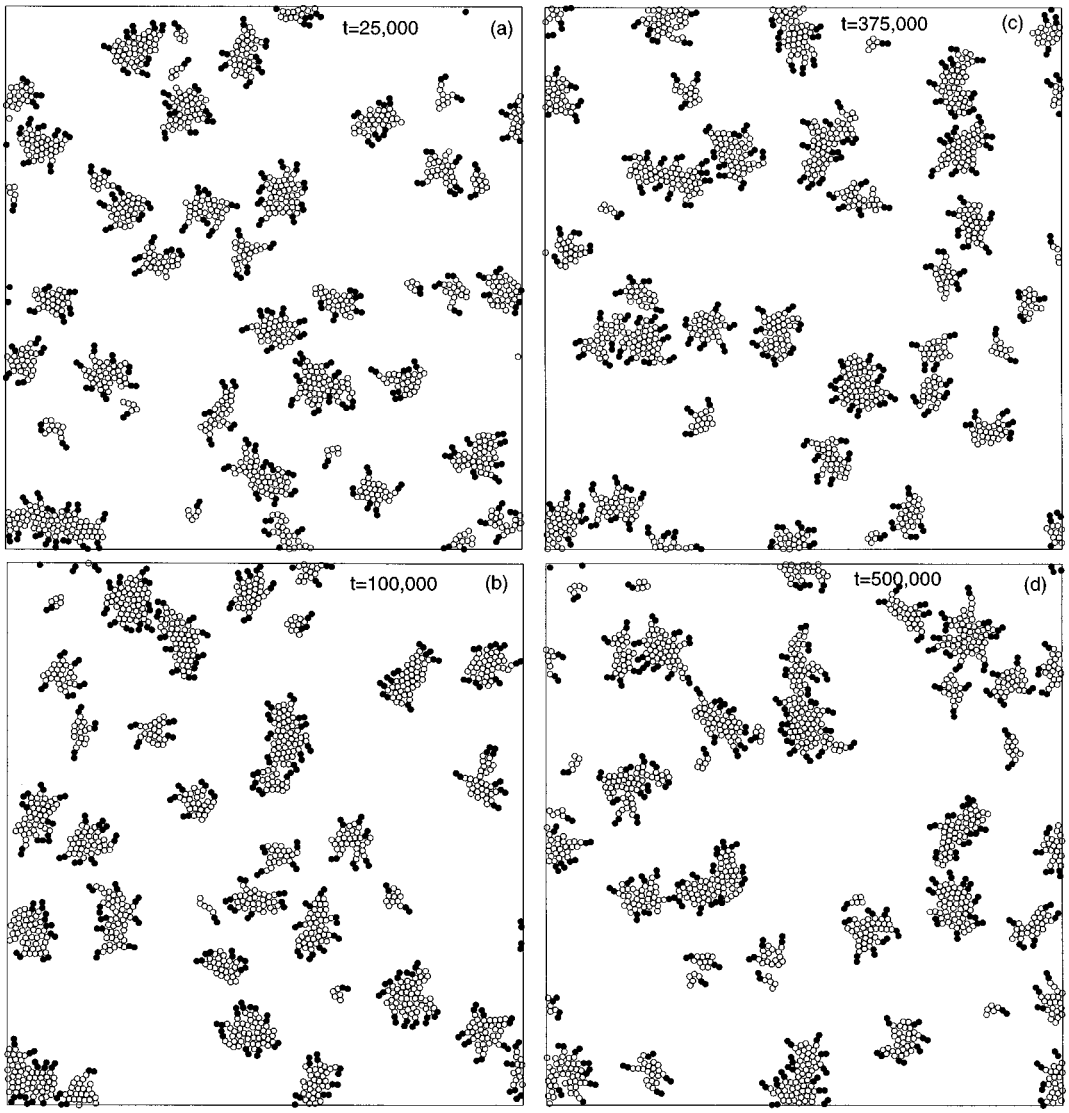

FIG. 4. Snapshots of surfactant aggregation at different time for parameters corresponding to Fig. 2(c).

choice of $\sigma_{ht}=1.5\sigma_{tt}$ to satisfy the usual average rule for the LJ particles. We have adjusted the bond length for the head to the first tail particle to be $1.5l_0$ as well.[38] The SC parameters that we have used are listed in Table II. We also introduce a second cutoff distance R_{ij}^{sc} for the SC interaction for numerical expediency. We have performed simulations for various values of the screening parameter κ. For a detail comparison with the neutral surfactant results we present results for the same concentration and choice of the LJ parameters corresponding to the Fig. 1(a) ($T=0.5$ and $R_b=0.2$). Figures 8(a) and 8(b) show the snapshots for $\kappa=0.5$ and 0.1, respectively, for $u_0=10.0$. With an increasing value of κ^{-1}, the screening length, an order begins to appear in the sense that the distribution for the average separation between the ionic micelles becomes narrower. To give a more quantitative answer we have calculated the time averaged structure factor $S(k)$ for these two cases and compared them with the structure factor for the neutral surfactants. Figure 9 shows these structure factors. Compared to the neutral surfactants the ionic surfactants exhibit sharper peaks with increasing value of κ^{-1}. We have checked that the k value for the peak corresponds to the average separation. This order is reminiscent of the two-dimensional ordering of a two-dimensional screened Coulomb gas right above its melting point. The algorithms that we use here either update a single monomer or one surfactant chain only. If we introduce *additional moves for the center of masses* for the micelles after they are formed we believe this local ordering will finally go over to a hexagonally ordered structure. To our knowledge this is a new result compared to the earlier work on micellar aggregation. Figure 10 shows cluster distributions corresponding to Fig. 8. We notice from Fig. 8 that the number of free surfactant chains is less compared to the neutral case at the same temperature [Fig. 1(a)]. It is likely that in presence of the screened Coulomb interaction the entropic contribution to the free energy is less for the surfactants. In presence of the SC interaction it becomes harder for the surfactants to move from one configuration to another one with the same energy. Therefore they take the alternate route to minimize the energy from the attractive tail-tail interactions.

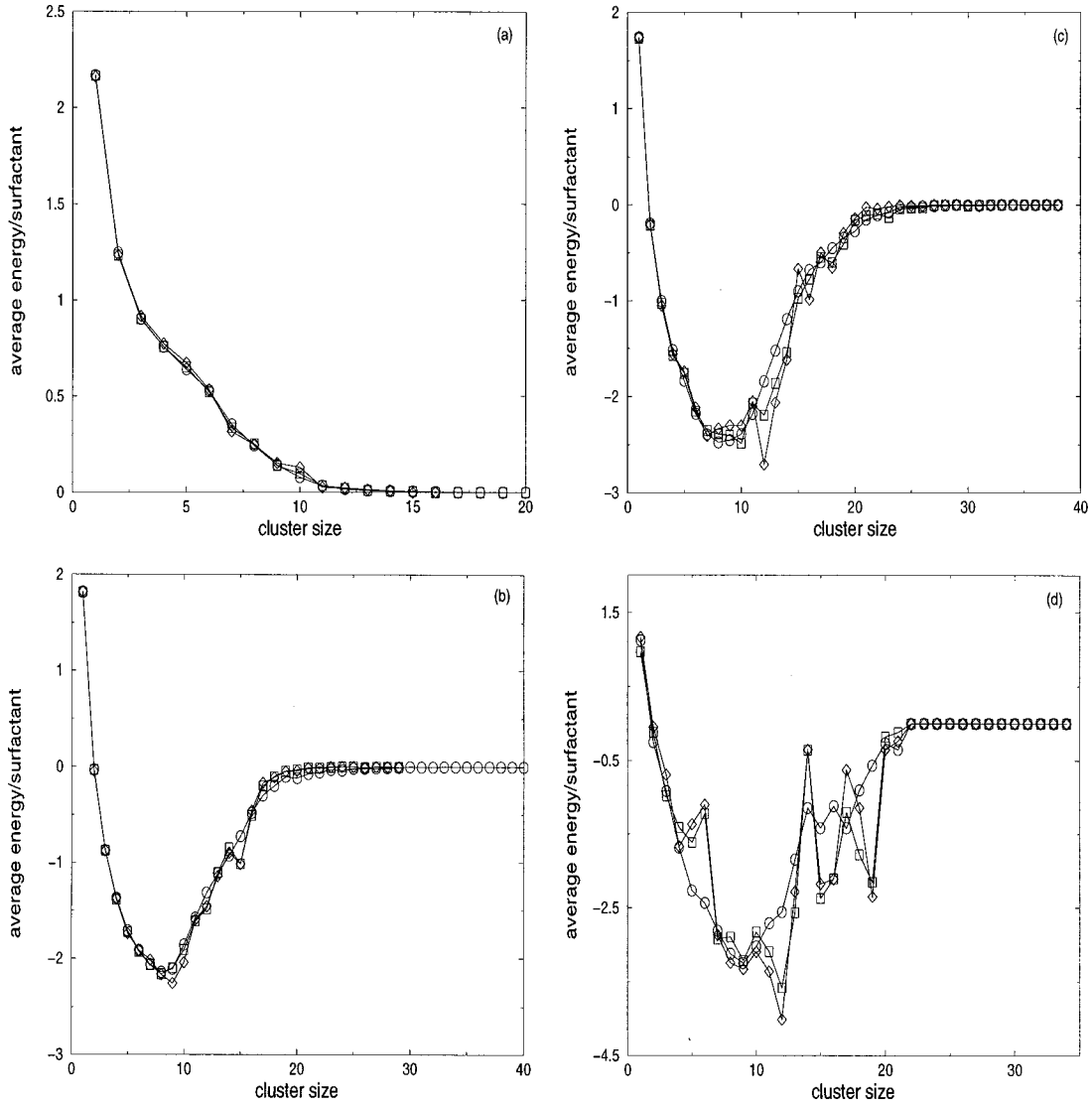

FIG. 5. $\tilde{E}_N \sim N$ for Figs. 2(a)–2(d). Circles represent the full time averaged distribution. Squares and diamonds represent time averaged distribution for the last 100 000 and 50 000 time steps. The ensemble average is also performed over different initial configuration.

E. Neutral surfactants and host particles

We now discuss the role of external host particles in aggregation of neutral surfactants. This brings us to the important issue of cooperative versus biomimetic pathway to obtain mesoporous sieves mentioned in the introduction.[11] In order to address this issue we have considered two possible simulation pathways. The first pathway is to start with a *preformed micellar arrangement* of surfactants [as shown in Fig. 1(a)] and allow inorganic host particles to interact with these micellar aggregates. In the second case, we start with a random configuration of the surfactant-host system. This second pathway corresponds to the cooperative self-assembly case. If one adds host particles at a stage when the surfactants have already self-assembled into micelles, then the host particles will either form aggregates among themselves, or they may encase these micelles to minimize the energy. This will depend on the interaction strengths,[39] ϵ_{hp} and ϵ_{pp}. A typical snapshot of this pathway is shown in Fig. 11. Here a choice of $\epsilon_{hp} > \epsilon_{pp}$ makes the host particles mostly decorate the micelles rather than forming clusters of their own. A choice of $\epsilon_{hp} = \epsilon_{pp} = 1$ will allow many host-particle aggregates along with isolated host particles in the system as shown in Fig. 11(b). We have checked that for a very large value of ϵ_{hp} host particles have more drastic effect on deforming the micelles.[26]

Now we discuss the configuration obtained for the cooperative self-assembly process. It is not *a priori* obvious that in the presence of the host particles from the very beginning, a random initial distribution of surfactants will evolve into micelles. Figure 12 demonstrates the existence of these alternate generalized biomimetic and less obvious route. Here also micellization proceeds unhindered and we obtain host-encased micelles for the same set of parameters as in Fig. 11. It should be noted here that the experimental pathways leading to such self-assembling structures are very diverse and complex. Depending on experimental conditions one may or may not obtain the same final structures by using two different pathways, even for the same surfactant-host stoichiom-

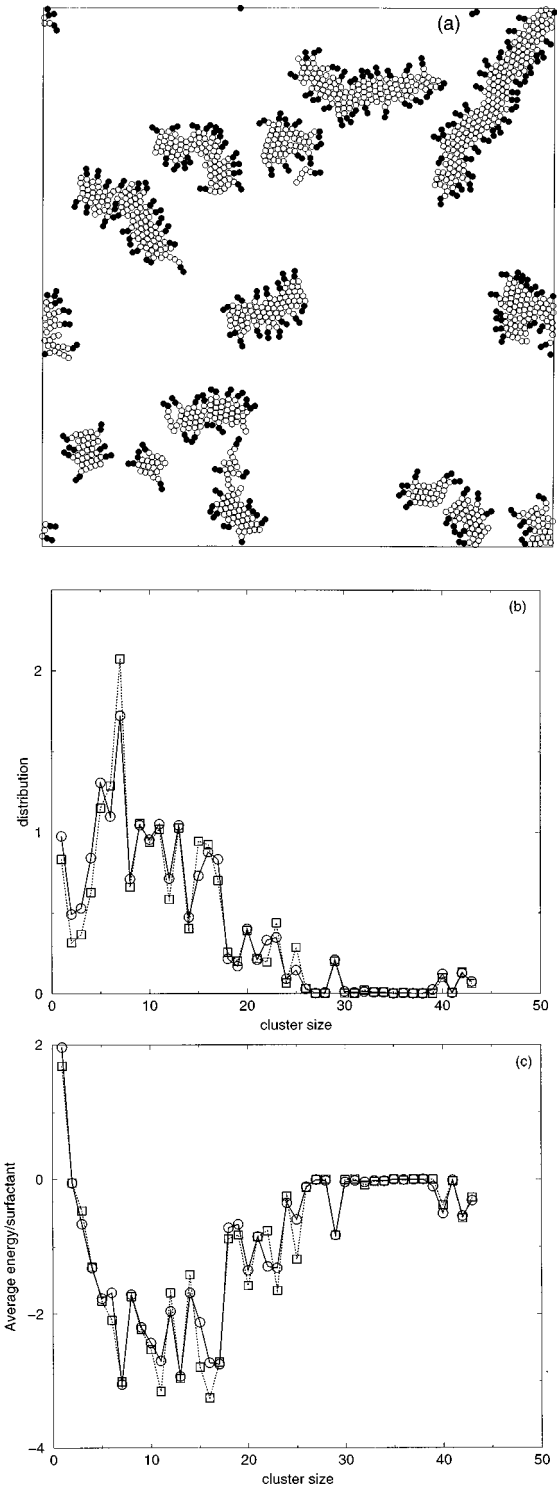

FIG. 6. (a) Snapshot of micellar aggregation for $R_b=0.6$ at $T=0.45$. (b) The corresponding cluster distribution, and (c) $\tilde{E}_N$ as a function of aggregation number N.

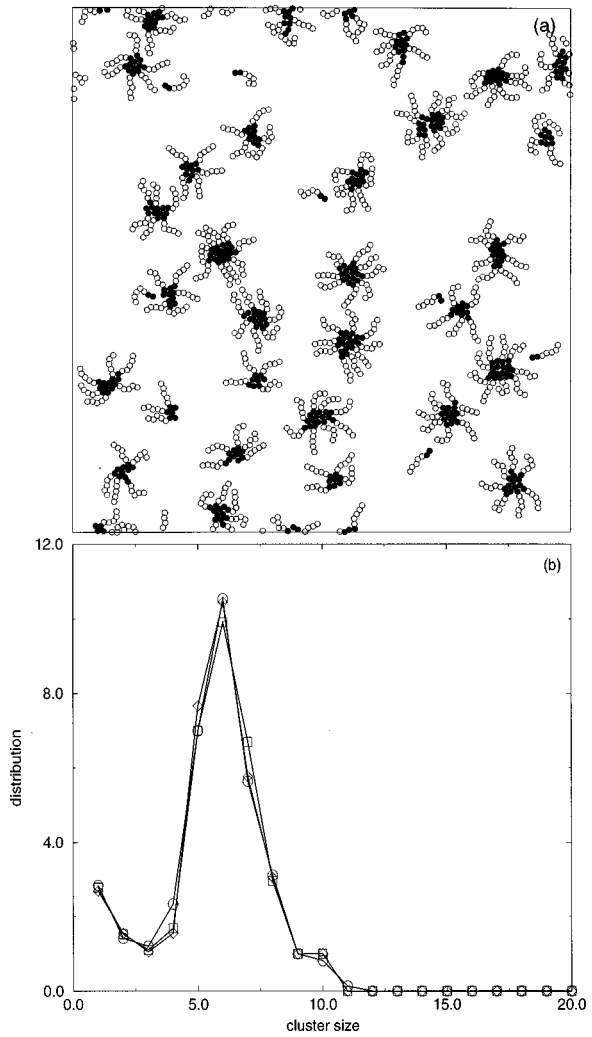

FIG. 7. (a) Snapshot of micellar aggregation and (b) the corresponding cluster distribution at $T=0.25$. The rest of the parameters are the same as in Fig. 1.

etry. It is exciting to note that this essential complexity is present in our simple model. As an example, we have included another snapshot of the cooperative self assembly process in Fig. 12(b) for the same set of parameters as in Fig. 12(a), but for a lower temperature ($T=0.25$). Instead of micellization we now get wormlike structures seen in some experiments.[40] It seems clear that this simple model has ample potential to predict new phases as a function of different parameters and concentrations. Such studies may contain information to promote further experiments.

IV. DISCUSSION AND SUMMARY

We have presented detailed numerical results for micellization of surfactants using off-lattice Monte Carlo method. An important ingredient of our method is that unlike many previous numerical studies we have eliminated the solvent degrees of freedom. The interaction of the surfactants with the solvent particles is implicit in the phenomenological parameters of the model. Since micellization occurs at low surfactant concentration, this method has a distinct computa-

TABLE II. Interaction parameters for the ionic surfactants.

Interaction	R_{ij}^c/σ_{ij}	σ_{ij}	ϵ_{ij}	κ	u_0	R_{ij}^{sc}
Head-head	$2^{1/6}$	2.0	1.0	0.1–0.5	5–10	10–30
Head-tail	$2^{1/6}$	1.5	1.0			
Tail-tail	2.5	1.0	1.0			

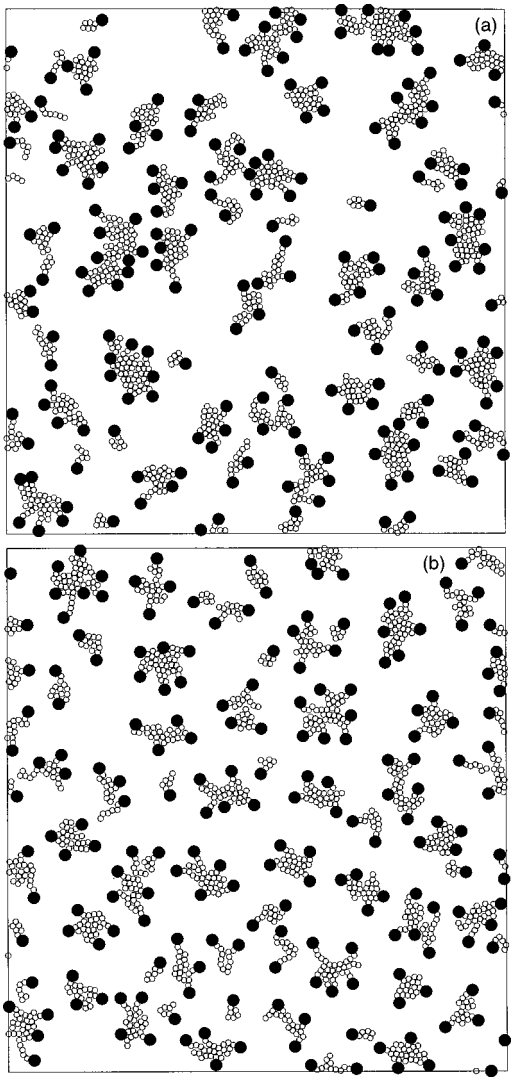

FIG. 8. (a) Snapshots of micellar aggregation for ionic surfactants at the end of MC time 500 000. The SC parameters are (a) $u_0=10.0$, $\kappa=0.5$, and $R_{hh}^{sc}=30.0$, (b) $u_0=10.0$, $\kappa=0.1$, and $R_{hh}^{sc}=30.0$, respectively. The rest of the parameters are the same as in Fig. 1.

tional advantage since no time is spent to monitor the solvent degrees of freedom. This helps us not only to study multimicelle systems for both ionic and nonionic surfactants but also the cooperative self-assembly of the surfactants in the presence of host particles. For statistical properties, e.g., cluster distribution and $\tilde{E}_N$, an ensemble averaging for different initial conditions was also feasible. First we consider neutral surfactants modeled via simple LJ interactions. For neutral micelles, the cluster-size distribution obtained from this simulation is qualitatively similar to previous studies where surfactant-solvent interactions are treated explicitly. This gives us confidence in our simplified yet computationally very efficient model. We demonstrated that the self-assembly of surfactants into inverted micelles is naturally embedded in this scheme. Next we extend these calculations for ionic surfactants. Here micellization occurs with additional ordering coming out of the longer range screened Coulomb interaction. We then study the role of additional host particles to mimic recent experiments on surfactant-silicate cooperative

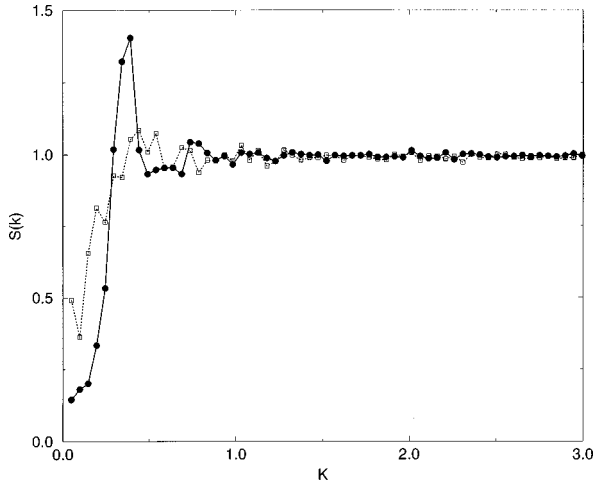

FIG. 9. Time averaged structure factors for neutral and ionic surfactants. The dashed line (squares) is for neutral surfactants whose typical snapshot is shown in Fig. 1(a). The solid line (circles) is for ionic surfactants whose typical configuration is shown in Fig. 8(b). The peak corresponds to the average separation among the micelles which is sharp and narrow due to the presence of screened Coulomb interaction. The time average is taken at every 500th step over the last 50 000 MC steps.

self-assembly. For certain parameter values we still obtain unhindered self-assembly of surfactants into host-encased micelles. We also note that the thickness of the walls and the shape of the encased micelles can be tailored by proper

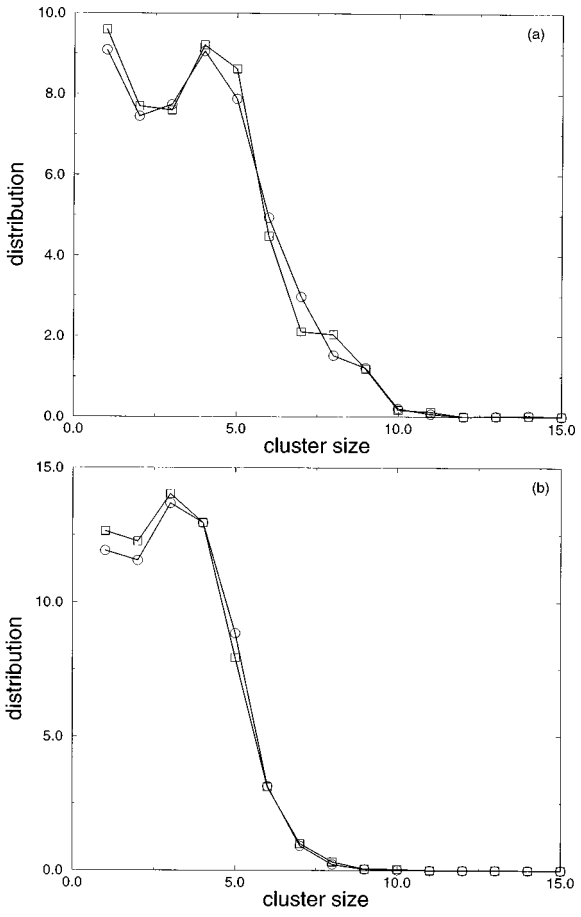

FIG. 10. Cluster distribution of ionic surfactants for Figs. 8(a) and 8(b).

TABLE III. Interaction parameters for the host particles.

Interaction	R_{ij}^c/σ_{ij}	σ_{ij}	ϵ_{ij}
Head-particle	2.5	1.0	1.0–2.0
Tail-particle	$2^{1/6}$	1.0	1.0
Particle-particle	2.5	1.0	1.0–2.0

choice of the parameters. These findings may have relevance to guide new experiments. Finally we demonstrated that introducing host particles on the preformed micellar phase one also obtains host encased micellar structures. This is consistent with recent experiments that the final configurations which are similar can be obtained via different pathways. A detailed study of inverted micelles along with the investigations of cooperative self-assembly of ionic micelles with host particles is currently under preparation which we will report in a separate publication.

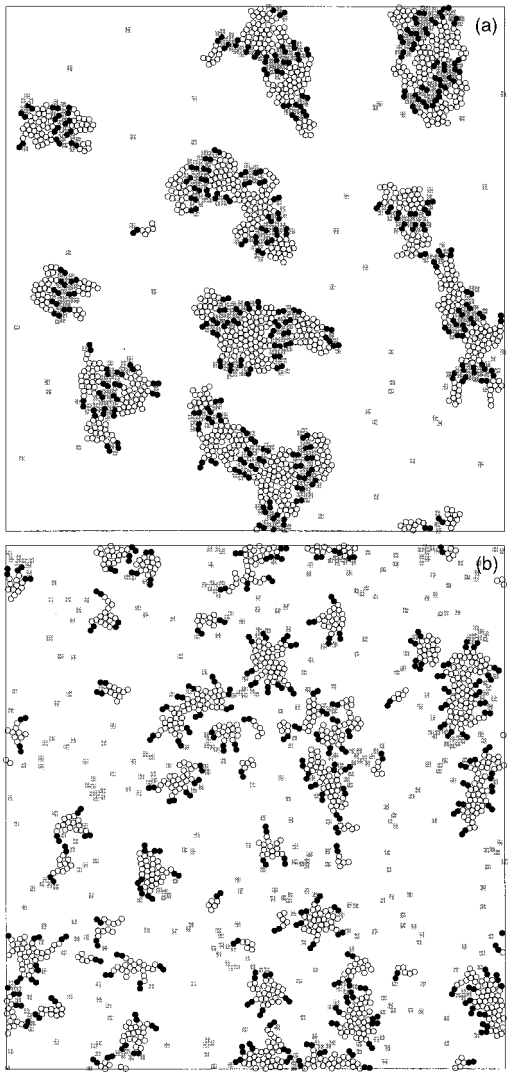

FIG. 11. Effect of host particles (shaded squares) on preformed micelles for the first pathway discussed in the text. Figure shows snapshot for 410 host particles for (a) $\epsilon_{pp}=1$, $\epsilon_{hp}=2$ and (b) $\epsilon_{pp}=1$, $\epsilon_{hp}=1$. The rest of the parameters are the same as in Fig. 1.

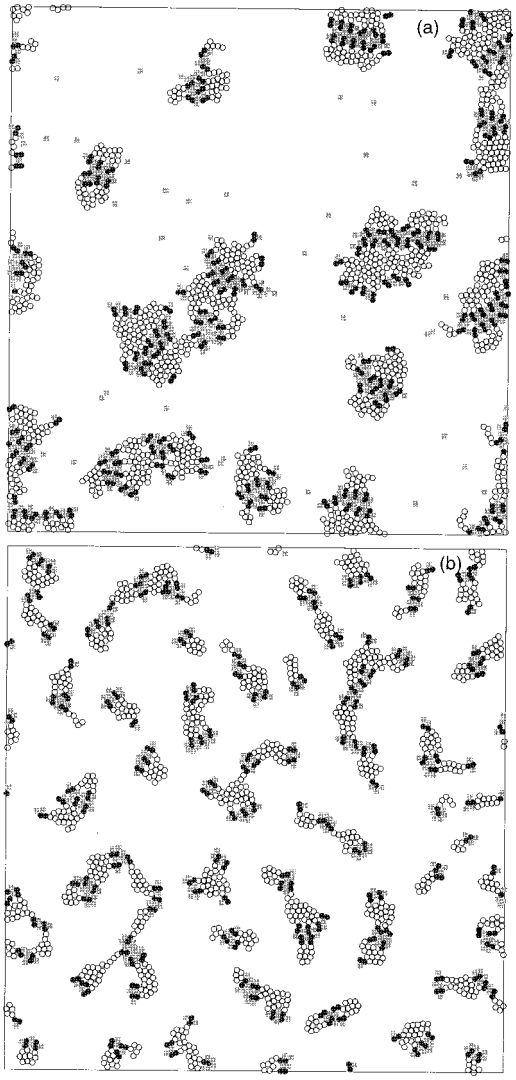

FIG. 12. Cooperative self-assembly for surfactant-host system for the second pathway mentioned in the text. Figure shows snapshots for (a) $\epsilon_{pp}=1$, $\epsilon_{hp}=2$, $T=0.5$, (b) $\epsilon_{pp}=1$, $\epsilon_{hp}=2$, $T=0.25$. Here the host particles are present from the very beginning of the self-assembly.

ACKNOWLEDGMENTS

We thank Dr. Eric Prouzet, Dr. Peter Tanev, and Dr. Zhen Wang for numerous discussions and bringing to our attention other experimental work. We especially thank Professor T. J. Pinnavaia for giving details of his work and for comments on our manuscript. This work has been supported by National Science Foundation Grant numbers CHE-9633798 (A.B. and S.D.M.), DMR-9413513 (A.C.). Partial computer support through Michigan State University is gratefully acknowledged. A.C. thanks Michigan State University for the hospitality shown during the present work.

[1] For reviews, see, *Surfactants in Solution*, edited by (a) K. L. Mittal and P. Bothorel (Plenum, New York, 1985) and (b) K. L. Mittal and B. Lindman (Plenum, New York, 1984), and other volumes in this series; *Physics of Amphiphiles: Micells, Vesicles and Microemulsions*, edited by V. DeGiorgio and M. Corti (North-Holland, Amsterdam, 1985).
[2] G. J. T. Tiddy, Phys. Rep. **57**, 1 (1980).
[3] C. Tanford, *The Hydrophobic Effect* (Wiley, New York, 1980).

[4] J. Israelachvili, *Intermolecular and Surface forces* (Academic, New York, 1985).
[5] *Physics of Complex and Supermolecular Fluids*, edited by S. A. Safran and N. A. Clark (Wiley, New York, 1987).
[6] R. G. Laughlin, *The Aqueous Phase Behavior of Surfactants* (Academic, New York, 1994).
[7] See articles in special issue of Sci. **277**, (1997).
[8] J. P. Chen, C. M. Sorensen, K. J. Klaubaude, and G. C. Hajipananjis, Phys. Rev. B **51**, 11527 (1995).
[9] C. T. Kresge, M. E. Leonowicz, W. J. Roth, J. C. Vertuli, and J. S. Beck, Nature (London) **359**, 710 (1992); Mark E. Davis, Proceedings of the MRS Spring Meeting Better Ceramics through Chemistry VI, 1994 (unpublished).
[10] Q. Huo, D. I. Margolese, U. Ciesla, D. G. Demuth, P. Feng, T. E. Gier, P. Seger, A. Firouzi, B. F. Chmelka, F. Schuth, and G. D. Stucky, Chem. Mater. **6**, 1176 (1994); Q. Huo, D. I. Margolese, U. Ciesla, P. Feng, T. E. Gier, D. G. Demuth, T. E. Gier, P. Seger, R. Leon, P. M. Petroff, A. Firouzi, F. Schuth, and G. D. Stucky, Nature (London) **368**, 317 (1994); A. Monnier, F. Schuth, Q. Huo, D. Kumar, D. Margolese, R. S. Maxwell, G. D. Stucky, M. Krishnamurty, P. Petroff, A. Firouzi, M. Janicke, B. M. Chmelka, Science **261**, 1299 (1993).
[11] J. S. Beck, J. C. Vertuli, W. J. Roth, M. E. Leonowicz, C. T. Kresge, K. D. Schmitt, C. T.-W. Chu, D. H. Olson, E. W. Sheppard, S. B. McCullen, J. B. Higgins, and J. L. Schlenker, J. Am. Chem. Soc. **114**, 10834 (1992).
[12] P. T. Tanev and T. J. Pinnavaia, Science **267**, 865 (1995); P. T. Tanev and T. J. Pinnavaia, Chem. Mater. **8**, 2068 (1996); also in *Access in Nanoporous Materials*, edited by T. J. Pinnavaia and M. F. Thorpe (Plenum, New York, 1995); G. S. Attard, J. C. Glyde, and C. J. Goltner, Nature (London) **378**, 366 (1995).
[13] K. M. McGrath, D. M. Dabs, N. Yao, I. A. Aksai, and S. M. Gruner, Science **277**, 552 (1997).
[14] S. Mann, Nature (London) **365**, 499 (1993); Science **261**, 1286 (1993).
[15] G. Gompper and M. Schick, *Phase Transition and Critical Phenomena, Vol. 16* (Academic, New York, 1994). An extensive lattice Monte Carlo work for the oil-water-surfactant system have been done by Larson (see Ref. 16).
[16] R. G. Larson, L. E. Scriven, and H. T. Davis, J. Chem. Phys. **83**, 2411 (1985); R. G. Larson, J. Chem. Phys. **89**, 1642 (1988); **91**, 2479 (1989); **96**, 7904 (1992); J. Phys. II France **6**, 1441 (1996).
[17] J. Israelachvili, D. J. Mitchell, and B. W. Ninham, J. Chem. Soc., Faraday Trans. 2 **72**, 1525 (1976); R. Nagarajan and E. Ruckenstein, Langmuir **7**, 2934 (1991).
[18] K. Watanabe and M. L. Klein, J. Phys. Chem. **93**, 6897 (1989); **95**, 4158 (1991).
[19] E. Egberts and H. J. C. Berendsen, J. Chem. Phys. **89**, 3715 (1988).
[20] J.-C. Desplat and C. M. Care, Mol. Phys. **87**, 441 (1994).
[21] C. J. Wijmans and P. Linse, Langmuir **11**, 3748 (1995); A. D. Mackie, A. Z. Panagiotopolous, and I. Szliefer, Langmuir **13**, 5022 (1997).
[22] D. R. Rector, F. van Swol, and J. R. Henderson, Mol. Phys. **82**, 1009 (1994).
[23] B. Smit, K. Esselink, P. A. Hilbers, N. M. van Os, L. A. M. Rupert, and I. Szleifer, Langmuir **9**, 9 (1993).
[24] B. Smit, P. A. Hilbers, K. Esselink, L. A. M. Rupert, and N. M. van Os, J. Chem. Phys. **95**, 6361 (1991).
[25] B. Palmer and J. Liu, Langmuir **12**, 746 (1996).
[26] B. Palmer and J. Liu, Langmuir **12**, 6015 (1996).
[27] J. Forsman and B. Jonsson, J. Chem. Phys. **101**, 5116 (1994), and references therein.
[28] Following Palmer *et al.* (Ref. 25), we have chosen a bending potential that favors 180° angles in the tail rather than 120° angles. This increases the effective length of the surfactants by preventing sharp bends in the tail. Also, as mentioned by Palmer *et al.* (Ref. 25), simulations indicate that 70%–80% of dihedral angles in the hydrocarbon tail are in the *trans* configuration, which supports the use of a straight tail.
[29] F. T. Wall and F. Mandel, J. Chem. Phys. **63**, 4592 (1975).
[30] P. H. Verdier and W. H. Stockmayer, J. Chem. Phys. **36**, 227 (1962).
[31] G. S. Grest, B. Dunweg, and K. Kremer, Comput. Phys. Commun. **55**, 269 (1989).
[32] D. Blankschtein, G. M. Thurston, and G. B. Benedek, Phys. Rev. Lett. **54**, 955 (1985); G. M. Thurston, D. Blankschtein, M. R. Fisch, and G. B. Benedek, J. Chem. Phys. **84**, 4558 (1986); D. Blankschtein, G. M. Thurston, and G. B. Benedek, *ibid.* **85**, 7268 (1986); S. Puvvada and D. Blankschtein, *ibid.* **92**, 3710 (1990).
[33] A. Ben-Shaul, I. Szleifer, and W. M. Gelbart, J. Chem. Phys. **83**, 3597 (1985); I. Szleifer, A. Ben-Shaul, and W. M. Gelbart, *ibid.* **83**, 3612 (1985).
[34] Actually for other type of repulsive of interactions, e.g., K/a^p, where $p>1$ the argument still holds good (Ref. 4).
[35] The value of the surfactant concentration 0.02 is certainly above critical micellar concentration. Our choice was guided partially by the earlier work of Rector *et al.* (Ref. 22) and from preliminary runs at several concentrations.
[36] We have tried to understand the physics from the quantity $\tilde{E}_N$. However, it is possible to calculate $\mu_N^0-\mu_1^0 \sim N$ [Eq. (10)] from the normalized cluster distribution. We have calculated $\mu_N^0-\mu_1^0$ from the cluster distribution data (X_i) obtained from our simulation and checked that the dependence of $\mu_N^0-\mu_1^0$ is a monotonically decreasing function of N, consistent with previous work (Ref. 21).
[37] Usually the ionic head surfactants have bigger heads compared to hydrocarbon tail particles.
[38] When the bond length becomes unequal on either side of a monomer the Eq. (4) for kink jump does not hold good. For the ith particle in a given chain and choosing the origin at the $i-1$ particle the generalized kink jump algorithm becomes $\theta \rightarrow -\theta$. Here $\theta=\cos^{-1}(\mathbf{d}_{i+1,i-1}\cdot\mathbf{d}_{i,j-1})/(|\mathbf{d}_{i+1,i-1}||\mathbf{d}_{i,i-1}|)$, and $\mathbf{d}_{i,j}$ is the vector along the bond from the ith to the jth monomer. For fixed bond lengths the above equation simplifies to Eq. (4) without going through the more expensive computation of the angle. We have incorporated these generalized kink jump moves for the tail particle next to the ionic head.
[39] Since one of our objectives is to look for host encased micellar aggregation a natural choice is to take the head-particle and particle-particle interactions attractive and choose tail-particle interaction to be repulsive ($R_{hp}^c=2.5\sigma_{hp}$, $R_{pp}^c=2.5\sigma_{pp}$, $R_{tp}^c=2^{1/6}\sigma_{tp}$).
[40] If one incorporates additional Monte Carlo moves for the clusters themselves, it is possible that the surfactant-host system may attain a different state. Here we have shown only the preliminary results for cooperative self-assembly. The details of the surfactant-host self-assembly are currently under preparation.